

Universal Octahedral-Site Distortion in Orthorhombic Perovskite Oxides

J.-S. Zhou and J. B. Goodenough

Texas Materials Institute, ETC 9.102, University of Texas at Austin, 1 University Station, C2201, Austin, Texas 78712, USA
(Received 14 October 2004; published 14 February 2005)

Lattice parameters of the orthorhombic perovskites RMO_3 (R = rare earth, M = Ti, V, . . . , Ni, and Ga) have been simulated based on the ionic M -O bond length and rigid $MO_{6/2}$ octahedra. Comparison with experimental data shows that the long-standing lattice-parameter anomaly generally found for the larger R^{3+} ions in these families is caused by a structural feature that is not revealed by the geometric tolerance factor widely used for the perovskites.

DOI: 10.1103/PhysRevLett.94.065501

PACS numbers: 61.50.Ah, 61.50.Ks, 61.66.Fn, 64.70.Kb

The AMX_3 perovskite structure consists of corner-shared $MX_{6/2}$ octahedra with larger A cations in a body-center position of higher anion coordination. The high density of this atomic arrangement makes the structure a common high-pressure phase; the structure also allows a large degree of freedom for mismatch between the equilibrium (A - X) and (M - X) bond lengths. Consequently, the AMX_3 oxides and fluorides with the perovskite structure are ubiquitous from the lower mantle of the earth to components of electronic devices.

Goldschmidt [1] introduced a tolerance factor

$$t \equiv (r_A + r_X)/\sqrt{2}(r_M + r_X),$$

to express the mismatch between the ambient (A - X) and (M - X) equilibrium bond lengths for a hard-ball model with ionic radii r obtained empirically from x-ray data. The bond-length mismatch created by a $t < 1$ is accommodated by cooperative rotations of the $MX_{6/2}$ octahedra; these rotations are accompanied by a corresponding shift of the A cations. Cooperative rotations can give rise to as many as 23 Glazer tilt systems [2]. The orthorhombic $Pbnm$ space group, which has the $a^-a^-b^+$ tilting system of Glazer notation, is the most common structure among the RMO_3 families having R = rare earth, M = transition metal, and a tolerance factor $t < 1$ [3,4]. As $(1 - t)$ decreases, the $MO_{6/2}$ tilting angle ω decreases; but a literature search showed no case where the orthorhombic phase changes smoothly to the cubic phase as $t < 1$ increases to $t = 1$. In all cases, an intermediate phase with a different tilting system appears between the orthorhombic and cubic phases. In this Letter, we point out that there is an additional A - X bond-length mismatch not considered by the Goldschmidt tolerance factor t that is *intrinsic* to the orthorhombic phase; it becomes increasingly operative as a $t < 1$ approaches $t = 1$ and is responsible for anomalies in the evolution of lattice parameters with t as well as for the observed phase transitions systematically observed.

In the orthorhombic perovskite structure with the $a^-a^-b^+$ tilting system, the cooperative rotations of the $MX_{6/2}$ octahedra are about a cubic $[110]$ axis, the $Pbnm$ orthorhombic b axis, to change the cubic lattice parameters from $a_0 \times a_0 \times a_0$ to $a \approx \sqrt{2}a_0 < b \approx \sqrt{2}a_0$ and $c =$

$2a_0$, as illustrated in Fig. 1. Given rigid octahedra rotating by an angle ω with an (M -O) bond length d , the calculated lattice parameters are $a = d\sqrt{8} \cos\omega$, $b = d[8(2 + \cos^2\omega)/3]^{1/2}$, and $c = d[48/(1 + 2 \sec^2\omega)]^{1/2}$. However, as pointed out by O'Keeffe and Hyde [5], perfect regularity of the octahedra is incompatible with fixed rotation axes, and the lattice parameters have been found to be extremely sensitive to octahedral-site distortions [3]. Woodward [6] has verified for several tilting systems that it is not possible to link together a three-dimensional network of perfectly rigid octahedra. However, neither this general argument nor the geometric relationship described by the t factor can account for why the octahedra become more distorted as the t factor increases smoothly to unity.

In order to demonstrate how the octahedral-site distortion evolves with the tolerance factor t , we compare in Fig. 2 the experimental lattice parameters taken from the literature with those calculated with the software program SPUDS [3] for several orthorhombic RMO_3 families (R = rare earth, M = the first-row transition metal or Ga). In

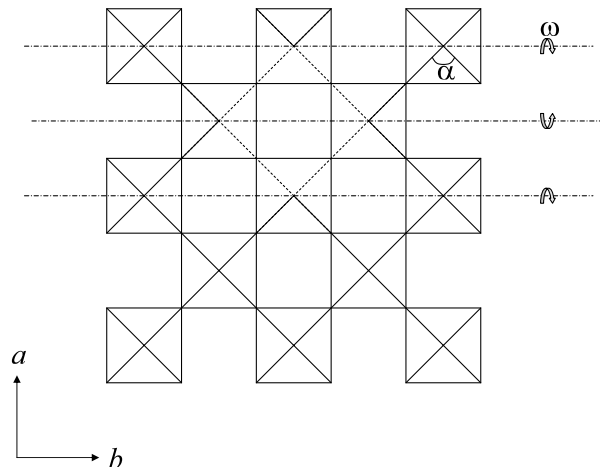


FIG. 1. Schematic drawing of the orthorhombic perovskite structure projected onto the a - b plane. The cubic perovskite unit cell is shown with dashed lines. O(2) is located at the corner of octahedra shown as a square in this plot. O(1) is at the apical position off the plane.

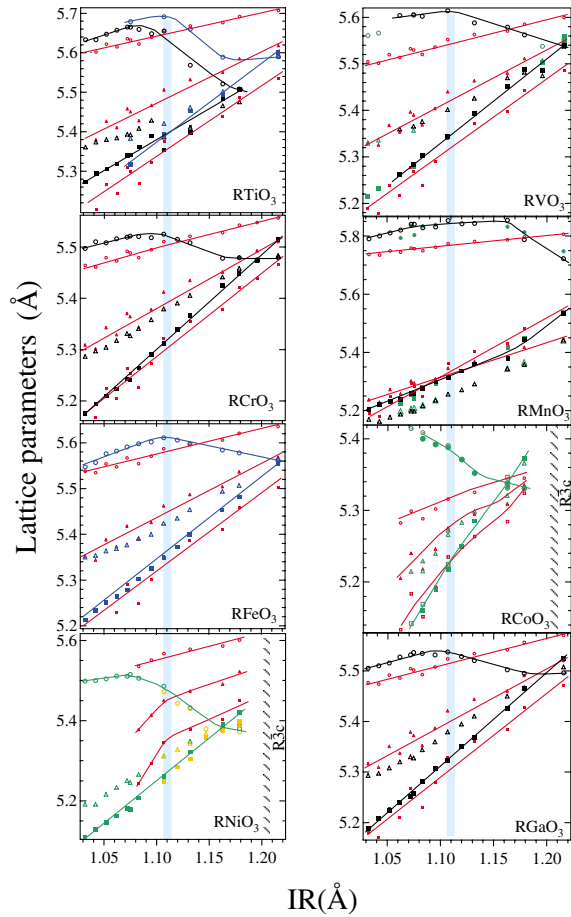


FIG. 2 (color). Lattice parameters versus ionic radius of the R^{3+} ion. Circles, triangles, and squares stand for b , $c/\sqrt{2}$, and a , respectively. The rare-earth radius in nine coordination is chosen since it is the highest coordination number available for all tabulated rare earths. Lines in the figure are a guide to the eyes. Points in red are calculated by SPuDS. All data shown in black are from Ref. [4]. The data from single-crystal diffraction are shown in blue. Data except for those in black are from Ref. [17] for $RTiO_3$, Refs. [18–22] for RVO_3 , Refs. [23,24] for $RMnO_3$, Refs. [25,26] for $RFeO_3$, Ref. [8,27] for $RCoO_3$, and Refs. [28–31] for $RNiO_3$.

each family, the M cation is unchanged and the tolerance factor t varies proportionally with the ionic radius of the R^{3+} ion (IR). Two important assumptions in the SPuDS calculation procedure make this comparison meaningful: (a) the bond lengths are determined by the bond-valence-sum rule and (b) the octahedra are kept rigid, i.e., six equivalent (M -O) distances and all O- M -O angles are 90° .

We highlight several important general features of Fig. 2 before discussing why some families behave slightly differently from the others. (1) The calculated parameters show the order $b > c/\sqrt{2} > a$ with all parameters increasing linearly with IR, which is consistent with the $a^-a^-b^+$ tilting system. This relationship applies qualitatively to most RMO_3 families of Fig. 2 and even quantitatively to those with $M = Ti, Cr, Fe,$ and Ga so long as the R^{3+} -ion radius is $IR < 1.11 \text{ \AA}$. The deviation near an $IR = 1.11 \text{ \AA}$ is most obvious in the b parameter. (2) Although the octahedral-site rotation angle ω of the $a^-a^-b^+$ tilting system remains finite, the deviation for $IR > 1.11 \text{ \AA}$ of the experimental b vs IR from that calculated leads to a pseudocubic phase with $b \approx a \approx c/\sqrt{2}$ in $LaTiO_3$, $LaVO_3$, $LaFeO_3$, and to even a $b < a$ in $LaCrO_3$ and $LaGaO_3$. Moreover, the equilibrium (M -O) bond lengths d do not change with the IR where $M = Ti, V, Cr, Mn, Fe,$ and Ga . As listed in Table I, whether a $b \approx a$ or a $b < a$ is reached in $LaMO_3$ depends on the equilibrium (M -O) bond length. (3) Although ω decreases with increasing IR, this reduction does not lead to a smooth transformation to the cubic perovskite structure; a phase transition to the rhombohedral $R\bar{3}c$ phase with the $a^-a^-a^-$ tilting system always occurs at the IR where the orthorhombic phase shows a $b < a$. In other words, the orthorhombic phase having a $b < a$ must be a precursor to the transition from a pseudocubic orthorhombic phase to the rhombohedral phase. This observation also leads to the prediction that a transition from the orthorhombic to the rhombohedral phase should occur at a tolerance factor t larger than that for the La^{3+} ion in $LaCrO_3$ and $LaGaO_3$. Structural studies at high temperature or under high pressure have demonstrated a transition to the rhombohedral phase in $LaCrO_3$ [10] and $LaGaO_3$ [11,12]. The t factor increases with temperature and pressure [13] in these cases. (4) These features clearly have a crystallographic origin since they apply to a broad range of orthorhombic perovskites that include both magnetic and diamagnetic insulators as well as Pauli paramagnetic metals. However, changes of electronic structure may alter these features, particularly where they involve a change with IR of the equilibrium (M -O) bond length. Therefore, we next consider the electronic configurations for $M = Ti, Mn, Co,$ and Ni .

The structure and physical properties of $RTiO_3$ are sensitive to the oxygen stoichiometry [14]. This sensitivity was not clarified in the ceramic samples prepared in earlier days, and the experimental lattice parameters shown as black circles for $RTiO_3$ in Fig. 2 are taken from early

TABLE I. The M -O bond length of RMO_3 from bond-valence-sum (BVS) and from the refinement of x-ray and neutron diffraction.

	Ti	V	Cr	Mn	Fe	Co	Ni	Ga
$(MO)_{BVS}(\text{\AA})$	2.047	2.0	1.98	2.03	2.015	1.89	2.006	1.98
$(MO)_{EXP}(\text{\AA})$	2.02–2.04	2.0–2.01	1.97 [7]	2.02	2.01	1.92 [8]	1.92–2.0	1.97 [9]

data. In the $R\text{MnO}_3$ family, a cooperative Jahn-Teller distortion of the $\text{MnO}_{6/2}$ octahedra is superimposed on the cooperative octahedral-site rotations; long and short O-Mn-O bonds alternate in the a - b planes and medium-length, regularly spaced O-Mn-O bonds along the c axis make $c/\sqrt{2} < a$; the orbital ordering enlarges significantly the orthorhombic strain parameter $s = (b - a)/(b + a)$, but the bonding is everywhere ionic and the SPUDS calculation is able to catch closely these features. The Co(III) ions of the $R\text{CoO}_3$ family undergo a thermally driven transition from a low-spin t^6e^0 state to intermediate-spin t^5e^1 and high-spin t^4e^2 states with increasing temperature. At room temperature, the population of higher spin states decreases as the IR is reduced. The resulting variation with IR of the mean size of the Co(III) ionic radius modifies the variation of the lattice parameters with IR in the $R\text{CoO}_3$ family. The $R\text{NiO}_3$ family shows the most significant discrepancy between the experimental and calculated variations of the lattice parameters with IR. The major cause of this discrepancy is a change in the mean equilibrium (Ni-O) bond length with changing character of the Ni-O-Ni bonding [15]. The SPUDS calculation does not take into account the changes in equilibrium Ni-O bond length with changing R^{3+} ion.

The bond-length mismatch responsible for a $t < 1$ is progressively relieved as IR increases. The agreement between the experimental and calculated lattice parameters for $\text{IR} < 1.11 \text{ \AA}$ shows that with the smaller R^{3+} ions the assumption of a rotation of rigid octahedra provides a good description of the orthorhombic perovskites. However, a collapse of b - a with increasing $\text{IR} > 1.11 \text{ \AA}$ and even a smooth crossover of b and a in some orthorhombic systems shows unambiguously that the octahedral sites become increasingly distorted as $\text{IR} > 1.11 \text{ \AA}$ increases. There are two ways that an octahedron can distort: The several (M -O) bond lengths may vary or the O- M -O bond angles may deviate from 90° . The parameter $\Delta_d \equiv (1/6)\sum_{n=1-6}[(d_n - \langle d \rangle)/\langle d \rangle]^2$ measures the magnitude of the variation of $d_\sigma = (M\text{-O})_\sigma$ bond lengths of an octahedral site; Δ_d has been shown [15] to decrease with increasing $\text{IR} < 1.08 \text{ \AA}$ in the $R\text{FeO}_3$ family where orbital ordering is not an issue. For this family, single-crystal diffraction data were available for all the rare-earth elements. In contrast to the evolution of Δ_d with IR, which shows retention of nearly uniform (Fe-O) bond lengths for all R^{3+} ions, the O(2)-Fe-O(2) bond angle $\alpha = 90^\circ \pm \delta$ undergoes an unambiguous decrease from 90° with increasing $\text{IR} > 1.12 \text{ \AA}$, see Fig. 3. Woodward *et al.* [16] have argued, in a study of the structure of $\text{Ln}_{0.5}\text{A}_{0.5}\text{MnO}_3$ ($A = \text{Sr}, \text{Ca}$), that the crossover of b and a may occur for a δ as small as 1° . It therefore appears that an increasing deviation of α from 90° occurs while the tilting angle ω decreases with increasing $\text{IR} > 1.11 \text{ \AA}$. Moreover, an octahedral-site distortion large enough to give an orthorhombic $b < a$ becomes unstable relative to a transition to

a rhombohedral $a^-a^-a^-$ tilting system that allows the A -site cation to have a larger near-neighbor anion coordination. *This intrinsic structural conflict is not reflected in the tolerance factor t and cannot be resolved by any structural distortion other than a first-order phase transition; it is a general phenomenon that systematically prevents a continuous evolution with increasing t from the orthorhombic to the cubic RMO_3 perovskite structure.*

Although the cause of the octahedral-site distortion deserves further investigation, its appearance at an IR larger than a common value of 1.11 \AA implies a resistance by the larger A -site cations to a reduction of the nearest-neighbor oxide-ion coordination. Consistent with this conclusion, Fig. 2 and Table I show that the smaller the equilibrium (M -O) bond length, the larger δ for a given R^{3+} ion. Interestingly, the bond-length variations at an octahedral site, which are induced by a cooperative Jahn-Teller orbital ordering and are incorporated into the orthorhombic distortion, allow the MO_3 array to accommodate a larger A -site cation without lowering α from 90° than in the case where all the (M -O) bond lengths are identical. For the $R\text{MnO}_3$ family, the SPUDS calculation, which includes the (Mn-O) bond-length variations but leaves $\alpha = 90^\circ$, matches the data up to an $\text{IR} = 1.16 \text{ \AA}$.

In conclusion, our structural analysis has revealed that the polyhedron formed by corner-shared $\text{MO}_{6/2}$ octahedra with the M -O bond length $d \approx 2.0 \text{ \AA}$ in the orthorhombic $a^-a^-b^+$ tilting system can accommodate only A -site R^{3+} cations with an $\text{IR} < 1.11 \text{ \AA}$ if $\text{MO}_{6/2}$ octahedra remain nearly rigid. Larger R^{3+} cations induce a deviation of 90° bond angles in the octahedral sites that decreases the b axis. Discovery of this additional structural bond-length mismatch helps to explain several long-standing problems in perovskites, i.e., the anomalous variation of the orthorhombic lattice parameters with the R^{3+} -ion IR, a general violation of Végard's law, and why the rhombohedral phase

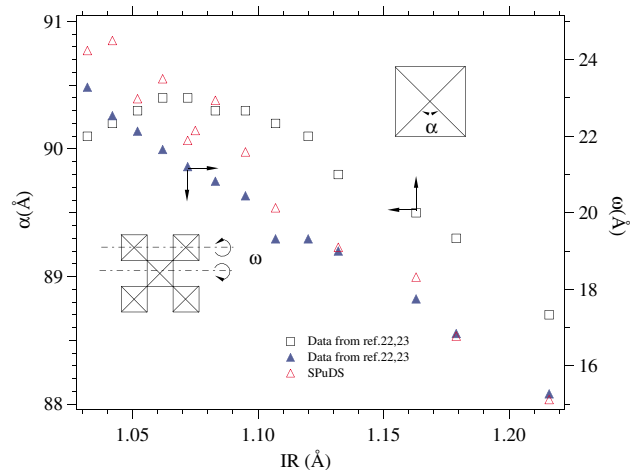


FIG. 3 (color online). Tilting angle ω and O- M -O angle α of octahedra versus IR for $R\text{FeO}_3$.

intervenes to prevent a smooth orthorhombic to cubic phase transition as would be expected from consideration of only the Goldschmidt tolerance factor.

We thank the NSF and the Robert A. Welch Foundation, Houston, TX, for financial support.

-
- [1] V. M. Goldschmidt, *Naturwissenschaften* **14**, 477 (1926).
[2] A. M. Glazer, *Acta Crystallogr. Sect. B* **28**, 3384 (1972).
[3] M. W. Lufaso and P. M. Woodward, *Acta Crystallogr. Sect. B* **57**, 725 (2001).
[4] J. B. Goodenough, and J. M. Longo, *Crystallographic and Magnetic Properties of Perovskite and Perovskite-Related Compounds*, in Landolt-Bornstein Tabellen, New Series III/4a, edited by K.-H. Hellwege (Springer-Verlag, Berlin, 1970), Chap. 3, p. 126.
[5] M. O'Keeffe and B. G. Hyde, *Acta Crystallogr. Sect. B* **33**, 3802 (1977).
[6] P. M. Woodward, *Acta Crystallogr. Sect. B* **53**, 32 (1997); **53**, 44 (1997).
[7] C. P. Khattak and D. E. Cox, *Mater. Res. Bull.* **12**, 463 (1977).
[8] X. Liu and C. T. Prewitt, *J. Phys. Chem. Solids* **52**, 441 (1991).
[9] L. Vasylechko, A. Matkovski, A. Suchocki, D. Savytskii, and I. Syvorotka, *J. Alloys Compd.* **286**, 213 (1999).
[10] T. Hashimoto, N. Matsushita, Y. Murakami, N. Kojima, K. Yoshida, H. Tagawa, M. Dokiya, and T. Kikegawa, *Solid State Commun.* **9**, 691 (1998).
[11] B. J. Kennedy, T. Vogt, C. D. Martin, J. B. Parise, and J. A. Hriljac, *J. Phys. Condens. Matter* **13**, L925 (2001).
[12] W. Marti, P. Fischer, F. Altorfert, H. J. Scheel, and M. Tadin, *J. Phys. Condens. Matter* **6**, 127 (1994).
[13] J. Zhao, N. L. Ross, and R. J. Angel, *Acta Crystallogr. Sect. B* **60**, 263 (2004).
[14] Y. Okada, T. Arima, Y. Tokura, C. Murayama, and N. Mori, *Phys. Rev. B* **48**, 9677 (1993).
[15] J.-S. Zhou and J. B. Goodenough, *Phys. Rev. B* **69**, 153105 (2004).
[16] P. M. Woodward, T. Vogt, D. E. Cox, A. Arulraj, C. N. R. Rao, and A. K. Cheetham, *Chem. Mater.* **10**, 3652 (1998).
[17] D. A. Maclean, H.-N. Ng, and J. E. Greedan, *J. Solid State Chem.* **30**, 35 (1979).
[18] R. T. A. Khan, J. Bashir, N. Iqbal, and M. N. Khan, *Mater. Lett.* **58**, 1737 (2004).
[19] P. Bordet, *J. Solid State Chem.* **106**, 253 (1993).
[20] A. Munoz, J. A. Alonso, M. T. Casais, M. J. Martinez-Lope, J. L. Martinez, and M. T. Fernandez-Diaz, *Phys. Rev. B* **69**, 144429 (2003).
[21] A. Munoz, J. A. Alonso, M. T. Casais, M. J. Martinez-Lope, J. L. Martinez, and M. T. Fernandez-Diaz, *J. Mater. Chem.* **13**, 1234 (2003).
[22] A. Munoz, J. A. Alonso, M. T. Casais, M. J. Martinez-Lope, J. L. Martinez, and M. T. Fernandez-Diaz, *Chem. Mater.* **16**, 1544 (2004).
[23] J. A. Alonso, M. J. Martinez-Lope, M. T. Casais, and M. T. Fernandez-Diaz, *Inorg. Chem.* **39**, 917 (2000).
[24] A. Waintal and J. Chenavas, *Mater. Res. Bull.* **2**, 819 (1967).
[25] M. Marezio and P. D. Dernier, *Mater. Res. Bull.* **6**, 23 (1971).
[26] M. Marezio, J. P. Remeika, and P. D. Dernier, *Acta Crystallogr. Sect. B* **26**, 2008 (1970).
[27] K. E. L. Mcllvried and G. J. McCarthy, PDF Cards No. 00-025-1054, No. 00-025-1057, No. 00-025-1073, and No. 00-025-1051.
[28] J. L. Garcia-Munoz, J. Rodriguez-Carvajal, P. Lacorre, and J. B. Torrance, *Phys. Rev. B* **46**, 4414 (1992).
[29] J. A. Alonso, M. J. Martinez-Lope, M. T. Casais, M. A. G. Aranda, and M. T. Fernandez-Diaz, *J. Am. Chem. Soc.* **121**, 4754 (1999).
[30] J. A. Alonso, M. J. Martinez-Lope, M. T. Casais, J. L. Garcia-Munoz, and M. T. Fernandez-Diaz, *Phys. Rev. B* **61**, 1756 (2000).
[31] J.-S. Zhou, J. B. Goodenough, and B. Dabrowski, *Phys. Rev. B* **70**, 81102 (2004).